

RESEARCH LETTER

10.1029/2018GL080074

Key Points:

- Summertime Adélie Land Bottom Water has a neodymium isotopic composition distinct from Ross Sea but similar to Weddell Sea Bottom Water
- Adélie Shelf Water is significantly less radiogenic and representative of the dense shelf waters exported in wintertime
- Regional differences in coastal geology are responsible for different isotopic fingerprints of Antarctic Bottom Water varieties

Supporting Information:

- Supporting Information S1

Correspondence to:

M. Lambelet,
m.lambelet@imperial.ac.uk

Citation:

Lambelet, M., van de Flierdt, T., Butler, E. C. V., Bowie, A. R., Rintoul, S. R., Watson, R. J., et al. (2018). The neodymium isotope fingerprint of Adélie Coast Bottom Water. *Geophysical Research Letters*, 45, 11,247–11,256. <https://doi.org/10.1029/2018GL080074>

Received 17 AUG 2018

Accepted 27 SEP 2018













Accepted article online 1 OCT 2018

Published online 16 OCT 2018

©2018. The Authors.

This is an open access article under the terms of the Creative Commons Attribution License, which permits use, distribution and reproduction in any medium, provided the original work is properly cited.

The Neodymium Isotope Fingerprint of Adélie Coast Bottom Water

M. Lambelet¹ , T. van de Flierdt¹ , E. C. V. Butler² , A. R. Bowie³ , S. R. Rintoul^{3,4,5} , R. J. Watson⁴ , T. Remenyi³ , D. Lannuzel^{3,6} , M. Warner⁷ , L. F. Robinson⁸ , H. C. Bostock⁹ , and L. I. Bradtmiller¹⁰ 

¹Department of Earth Science and Engineering, Imperial College London, London, UK, ²Australian Institute of Marine Science, Casuarina, Northern Territory, Australia, ³Antarctic Climate and Ecosystems Cooperative Research Centre, Hobart, Tasmania, Australia, ⁴CSIRO Oceans and Atmosphere, Hobart, Tasmania, Australia, ⁵Centre for Southern Hemisphere Oceans Research, Hobart, Tasmania, Australia, ⁶Institute for Marine and Antarctic Studies, University of Tasmania, Hobart, Tasmania, Australia, ⁷School of Oceanography, University of Washington, Seattle, WA, USA, ⁸School of Earth Sciences, University of Bristol, Bristol, UK, ⁹National Institute for Water and Atmospheric Research, Wellington, New Zealand, ¹⁰Department of Environmental Studies, Macalester College, Saint Paul, MN, USA

Abstract Adélie Land Bottom Water (ALBW), a variety of Antarctic Bottom Water formed off the Adélie Land coast of East Antarctica, ventilates the abyssal layers of the Australian sector of the Southern Ocean as well as the eastern Indian and Pacific Oceans. We present the first dissolved neodymium (Nd) isotope and concentration measurements for ALBW. The summertime signature of ALBW is characterized by $\epsilon_{\text{Nd}} = -8.9$, distinct from Ross Sea Bottom Water, and similar to Weddell Sea Bottom Water. Adélie Land Shelf Water, the precursor water mass for wintertime ALBW, features the least radiogenic Nd fingerprint observed around Antarctica to date ($\epsilon_{\text{Nd}} = -9.9$). Local geology around Antarctica is important in setting the chemical signature of individual varieties of Antarctic Bottom Water, evident from the shelf water signature, which should be considered in the absence of direct wintertime observations.

Plain Language Summary To understand the evolution of water masses back in time and elucidate the Southern Ocean's role in past climate change requires proxy data. Neodymium isotopes are commonly used but need to be better characterized in the modern ocean and especially where bottom water formation occurs. Adélie Land Bottom Water (ALBW) is a variety of Antarctic Bottom Water formed off the Adélie Land coast of East Antarctica. It ventilates the abyssal layers of the Australian sector of the Southern Ocean as well as the eastern Indian and Pacific Oceans. We present the first direct seawater analyses for Nd isotopes and concentrations in the Australian sector of the Southern Ocean. Our data reveal a distinctively unradiogenic signature of waters on the Adélie Land Shelf, precursor of ALBW, and show that the summertime signature of ALBW is distinct from Ross Sea Bottom Water and similar to Weddell Sea Bottom Water. Antarctic Bottom waters are not uniform around the continent and carry Nd isotope fingerprints characteristic of their formation area (local geology). This makes these water masses traceable back in time and is hence important for paleoceanography and for the study of past climate change.

1. Introduction

Antarctic Bottom Water (AABW) forms at discrete locations around the Antarctic margin. It supplies the lower limb of the global overturning circulation, ventilating the global ocean and affecting marine biogeochemical cycles (Marinov et al., 2006; Marshall & Speer, 2012; Orsi et al., 1999). Traditionally, most AABW studies have focused on the Ross Sea and the Weddell Sea, but other areas are increasingly discussed (Ohshima et al., 2013; Rintoul, 1998). A significant source of AABW is found off the Adélie Land coast, East Antarctica (Gordon & Tchernia, 1978; Orsi et al., 1999; Rintoul, 1998). It fills the bottom of the Australian sector of the Southern Ocean (Aoki et al., 2005) and, together with Ross Sea Bottom Water (RSBW), constitutes the main bottom water variety exported to the eastern Indian and Pacific oceans (Fukamachi et al., 2010; Mantyla & Reid, 1995; Nakano & Sugimotohara, 2002). Recent studies have documented changes in physical properties of Adélie Land Bottom Water (ALBW) linked to global climate change (Rintoul, 2018; van Wijk & Rintoul, 2014).

Inferring the composition of water masses back in time to elucidate the Southern Ocean's role in climate change requires proxy data. One commonly utilized proxy to constrain past water mass compositions and

ocean circulation is the neodymium (Nd) isotopic composition of seawater, expressed as ϵ_{Nd} (deviation of a measured $^{143}\text{Nd}/^{144}\text{Nd}$ ratio from the chondritic uniform reservoir in parts per 10,000; Jacobsen & Wasserburg, 1980). Neodymium is a lithogenic element, and in the modern ocean, seawater acquires its Nd isotopic composition at the interface of the ocean and the solid earth (Lacan & Jeandel, 2005a, 2005b). This is particularly relevant in the case of the Southern Ocean, where bottom waters are formed in areas proximal to different continental source lithologies and ages (Orsi et al., 1999; Roy et al., 2007). Away from continental margins, the Nd isotopic composition of seawater can trace water mass provenance and mixing (Lambelet et al., 2016).

Dissolved neodymium isotope data for Southern Ocean waters are scarce, particularly for AABW (van de Flierdt et al., 2016). The existing published studies contain 194 measurements for the whole Atlantic sector (Garcia-Solsona et al., 2014; Jeandel, 1993; Piepgras & Wasserburg, 1982; Stichel, Frank, Rickli, & Haley, 2012; Stichel, Frank, Rickli, Hathorne, et al., 2012) and 183 for the Pacific sector (Basak et al., 2015; Carter et al., 2012; Molina-Kescher et al., 2014; Rickli et al., 2014). No published data exist for the Indian Ocean sector.

We report the first results on dissolved Nd isotopic compositions and concentrations from the Australian sector of the Southern Ocean and the first data on the Nd isotope fingerprint of ALBW.

2. Samples and Methods

Four profiles of three to four depths were collected for dissolved Nd concentrations and isotopes on the RSV *Aurora Australis* during the IPY CASO-GEOTRACES SR3 cruise that took place from Hobart (Tasmania) to Antarctica along the $\sim 140^\circ\text{E}$ meridian between March and April 2008 (Figures 1 and S1 and Table S1 in the supporting information). Additionally, two profiles of six depths were collected for combined dissolved radionuclide and Nd isotope work on the RV *Tangaroa* during the MacRidge 2, TAN 0803 voyage from Wellington (New Zealand) to the polar front (PF) along 170°E between March and April 2008 (Figures 1 and S1 and Table S1). Methods for dissolved Nd concentration and isotope analyses are detailed in supporting information Text S1 and followed standard procedures in the MAGIC laboratories at Imperial College London (Auro et al., 2012; Crocket et al., 2014; Lambelet et al., 2016; Struve et al., 2016; Tanaka et al., 2000).

3. Results: Dissolved Nd Isotopes and Concentrations in the Context of Hydrography

The frontal structure south of Tasmania has been discussed by Sokolov and Rintoul (2002, 2007). We use the criteria from Table 6 of Sokolov and Rintoul (2002) to define the locations of the major fronts at the time of the 2008 survey. The fronts of the Southern Ocean separate distinct oceanographic regimes. The Subtropical Front (STF), the boundary between subtropical and subantarctic waters, is located near 46.6°S (Figure 1). Although the Subantarctic Front (SAF) is often split into two or three branches near 140°E (Sokolov & Rintoul, 2002, 2007, 2009), it formed a single broad frontal zone between 51.1°S and 52.5°S in March–April 2008. The northern limit of the SAF zone at 51.1°S and southern limit at 52.5°S coincide with the northern and southern branches of the SAF defined by Sokolov and Rintoul (2002). The northern branch of the PF (PF-N) flows eastward across the section at 58.7°S , meanders back to the west to cross the section near 56.2°S , then turns eastward to cross the section a third time at 53.9°S . The southern branch of the PF (PF-S) crosses the section near 60.1°S . The northern branch of the southern Antarctic Circumpolar Current (ACC) front (SACCF-N) is located near 62.6°S , while the southern branch of the SACCF is found near 63.5°S . The Southern Boundary at 64.7°S marks the southern limit of ACC waters.

Based on these frontal positions, station SR3-60 (48°S) lies between the SAF and the STF, and SR3-42 (52.67°S) is on the southern flank of the SAF (Figure 1). SR3-7 (65.43°S) and SR3-4 (65.80°S) were both located well south of the ACC regime, over the Antarctic slope and continental shelf, respectively.

The Macquarie Ridge acts as a topographic barrier with respect to the ACC (Rintoul et al., 2014; Smith et al., 2013). Therefore, large fractions of the currents flow through gaps in the ridge, leading to different front locations for TAN samples in comparison to the SR3 transect (Rintoul et al., 2014; Smith et al., 2013). Station 41 was situated between the SAF and the STF, whereas station 125 was sampled just south of the PF (Figure 1a).

The prominent water masses in the area are illustrated in Figures 1b and 1c and described below from surface to bottom, including hydrographic characteristics and Nd concentration and isotope results.

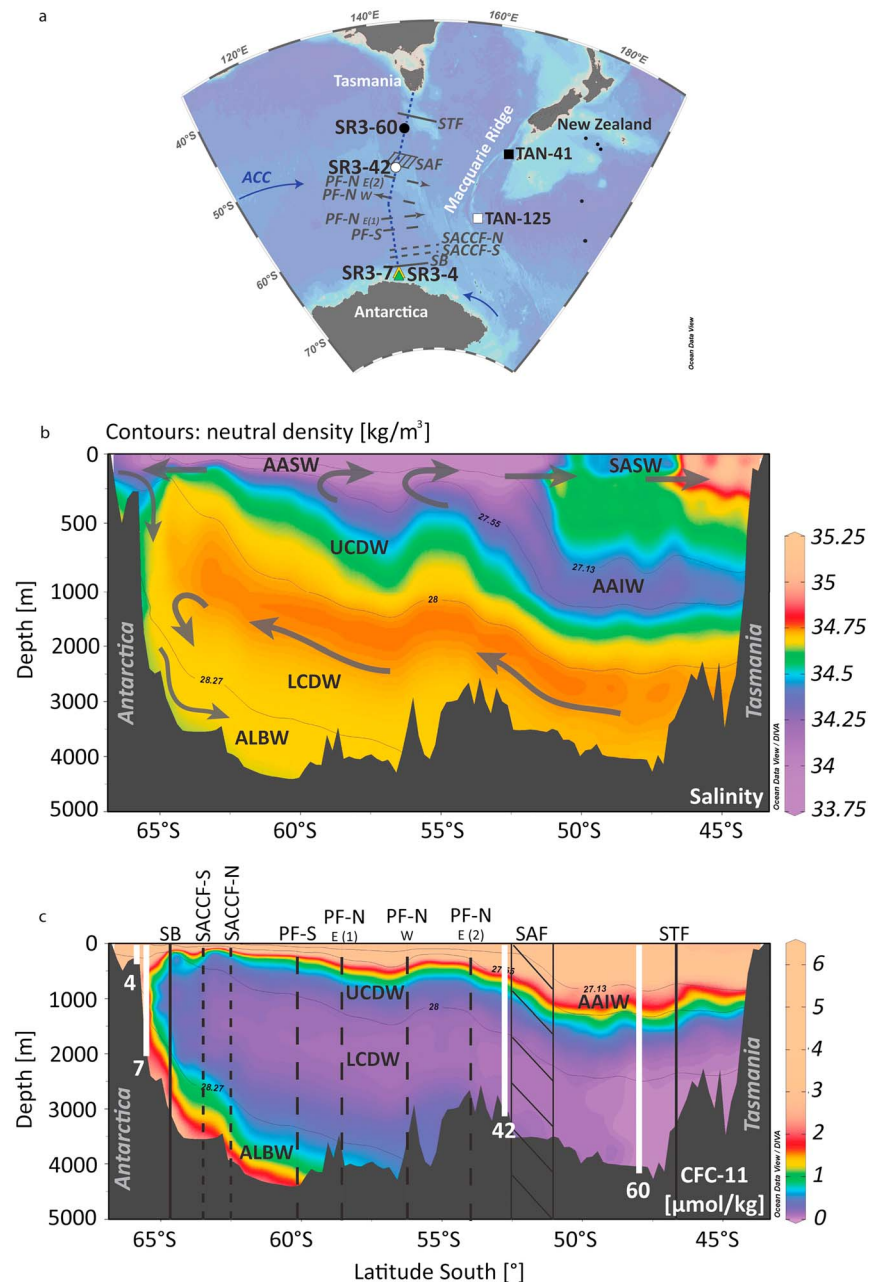


Figure 1. (a) Map of the sampling area. Black square: station TAN-41; white square: TAN-125; large black dot: SR3-60; large white dot: SR3-42; yellow triangle: SR3-7; green triangle: SR3-4. Small black dots: seawater profiles from the literature (Basak et al., 2015; Molina-Kescher et al., 2014). Blue dotted line from Tasmania to Antarctica: SR3 cruise track. Major fronts crossing the section at the time of the 2008 survey are depicted in dark gray. Main eastward flow of the Antarctic Circumpolar Current (ACC) represented by a curved blue arrow. Blue arrow near Antarctica: westward flow south of the ACC. Sections of salinity (b) and CFC-11 concentrations (c) for the SR3 survey realized using data from the GEOTRACES Intermediate Data Product 2014 (Mawji et al., 2015). The black lines represent neutral densities γ_n 27.13, 27.55, 28.0, and 28.27 kg/m^3 defining the major water mass boundaries (see section 3). Arrows in panel (b): schematic view of the meridional overturning circulation in the Southern Ocean, adapted from Rintoul et al. (2001). Black lines in panel (c): approximate major frontal locations. White lines in panel (c): SR3 Nd station locations. SASW = Subantarctic Surface Water; AASW = Antarctic Surface Water; AAIW = Antarctic Intermediate Water; UCDW = Upper Circumpolar Deep Water; LCDW = Lower-CDW; ALBW = Adélie Land Bottom Water; STF = Subtropical Front; SAF = Subantarctic Front; PF-N E(1) = northern branch of the polar front (eastward); PF-N W = northern branch of the PF (westward); PF-N E(2) = northern branch of the PF (eastward, crossing section a third time); PF-S = southern branch of the PF; SACCF-N = northern branch of the Southern ACC Front; SACCF-S = southern branch of the Southern ACC Front; SB = Southern Boundary of the ACC; CFC = chlorofluorocarbon. Map and sections created using ODV software (Schlitzer, 2012).

Subantarctic Surface Water is a relatively warm ($\theta = 4\text{--}14\text{ }^{\circ}\text{C}$) and fresh ($S = 33.5$ to 34.0) surface water situated south of the STF and north of the PF (Orsi et al., 1995), with neutral density $< 27.0\text{ kg/m}^3$. Three samples were collected in this water mass, characterized by ϵ_{Nd} between -10.2 and -8.7 , and $[\text{Nd}] = 7.5\text{ pmol/kg}$ (Table S1).

Antarctic Surface Water features very low temperatures, reaching down to the freezing point of $-1.9\text{ }^{\circ}\text{C}$, low salinities ($S = 33.5$ to 34.0) due to ice melting in summer (Tomczak & Godfrey, 2005), and neutral density $< 27.0\text{ kg/m}^3$. This water mass extends with rather uniform properties from the PF to the continental margin of Antarctica, where shelf waters are found at near freezing temperatures (Orsi et al., 1995). One sample was collected in this water mass, with $\epsilon_{\text{Nd}} = -8.1 \pm 0.3$ (Table S1).

Antarctic Intermediate Water is formed by subduction of Antarctic Surface Water at the SAF in the southeast Pacific and southwest Atlantic Ocean, with smaller quantities at other discrete locations around the Southern Ocean (e.g., Chiswell et al., 2015; Hartin et al., 2011; Sloyan & Rintoul, 2001). It is characterized by a salinity minimum north of the SAF (Figure 1b) and a neutral density from 27.13 to 27.55 kg/m^3 (Rintoul & Bullister, 1999; Rintoul et al., 2001; Sokolov & Rintoul, 2002). Three samples were collected in this water mass, featuring ϵ_{Nd} between -8.3 and -7.9 and $[\text{Nd}] = 9.9$ and 10.4 pmol/kg (Table S1).

Upper Circumpolar Deep Water (UCDW) is characterized by an oxygen minimum indicative of oxygen-poor waters entering the Southern Ocean from the deep Indian and Pacific basins and is found in the density range $27.55 < \gamma_n < 28.0\text{ kg/m}^3$ (Rintoul et al., 2001). *Lower Circumpolar Deep Water (LCDW)* has a slightly greater density ($28.0 < \gamma_n < 28.27\text{ kg/m}^3$) and high salinities due to influx of North Atlantic Deep Water (NADW; Orsi et al., 1995; Rintoul et al., 2001). In the present study, UCDW was present at three stations (SR3-42, TAN-41, and TAN-125) and was characterized by $\theta = 2.5 \pm 0.2\text{ }^{\circ}\text{C}$, $S = 34.54 \pm 0.23$ (2sd, $n = 3$), Nd isotopic compositions from -8.8 to -7.6 , and $[\text{Nd}] = 14.1\text{ pmol/kg}$ (Table S1). Lower Circumpolar Deep Water (CDW) was sampled at all four open ocean stations and features $\theta = 1.2 \pm 0.9\text{ }^{\circ}\text{C}$, $S = 34.72 \pm 0.03$, $\epsilon_{\text{Nd}} = -8.8 \pm 1.0$ ($n = 10$), and $[\text{Nd}] = 18.1$ to 32.6 pmol/kg ($n = 4$; Table S1). Both UCDW and LCDW outcrop south of the ACC (Figure 1b), where they contribute to the formation of surface and bottom waters, respectively, providing the principal connection between the upper and lower parts of the global overturning circulation (Marshall & Speer, 2012).

Antarctic Bottom Water (AABW), the densest water in the abyssal ocean, is formed at different locations on the shelf of the Antarctic continent, including the Weddell Sea, the Ross Sea, and the Adélie Coast (Orsi et al., 1999). Bottom topography restricts the exchange of AABW between the Atlantic, Pacific and Indian sectors of the Southern Ocean. Therefore, the bottom water in each basin reflects the properties of the local sources (Orsi et al., 1999). The Australian sector of the Southern Ocean is ventilated by two varieties of AABW: RSBW advected from the east, and ALBW formed along the Adélie-Wilkes Land Coast (Rintoul & Bullister, 1999; Williams et al., 2010). Rintoul (1998) showed that the high salinity signature of RSBW was not detectable at 140°E , due to influx of ALBW between 140°E and 148°E ; this statement holds for the 2008 SR-3 expedition (Table S1).

Adélie Land Bottom Water is cold ($-0.8\text{ }^{\circ}\text{C} < \theta < -0.4\text{ }^{\circ}\text{C}$), fresh ($34.62 < S < 34.68$) and dense ($\gamma_n > 28.27\text{ kg/m}^3$), and due to its recent exposure to the atmosphere, it has a high concentration of oxygen and chlorofluorocarbons (CFCs; Figure 1c and Table S1; Orsi et al., 1999; Rintoul & Bullister, 1999). The properties of ALBW reflect mixing between dense shelf waters exported in wintertime and modified CDW (mCDW) over the continental slope. In this study, the density range of ALBW was sampled only at station SR3-7 on the Antarctic slope, and the CFC data show that it is composed of 25% shelf water and 75% mCDW. Modified CDW is a mixture involving CDW featuring the same density as the regional variety of CDW found offshore, but it is colder and found on the shelf or slope (Whitworth et al., 1998). No Nd isotopes samples were collected from mCDW in the present study. ALBW features $\epsilon_{\text{Nd}} = -9.5$ to -8.6 , and $[\text{Nd}] = 23.2$ to 25.5 pmol/kg ($n = 3$; Figure 2 and Table S1).

Adélie Shelf Water was sampled at station SR3-4 situated on the continental shelf and is cold ($\theta < -1.3\text{ }^{\circ}\text{C}$), fresh ($S < 34.48$), and oxygen rich ($> 280\text{ }\mu\text{mol/kg}$). This water mass represents summer shelf water. Winter cooling and salinification during sea ice formation converts it to dense shelf water, the precursor to ALBW. It is characterized by a neutral density $< 28.27\text{ kg/m}^3$, a very negative Nd isotopic composition ($\epsilon_{\text{Nd}} = -10.5$ to -9.3), and Nd concentrations between 17.9 pmol/kg at the surface (6 m) to 21.0 pmol/kg close to the ocean seafloor (321 m; Figure 2a and Table S1).

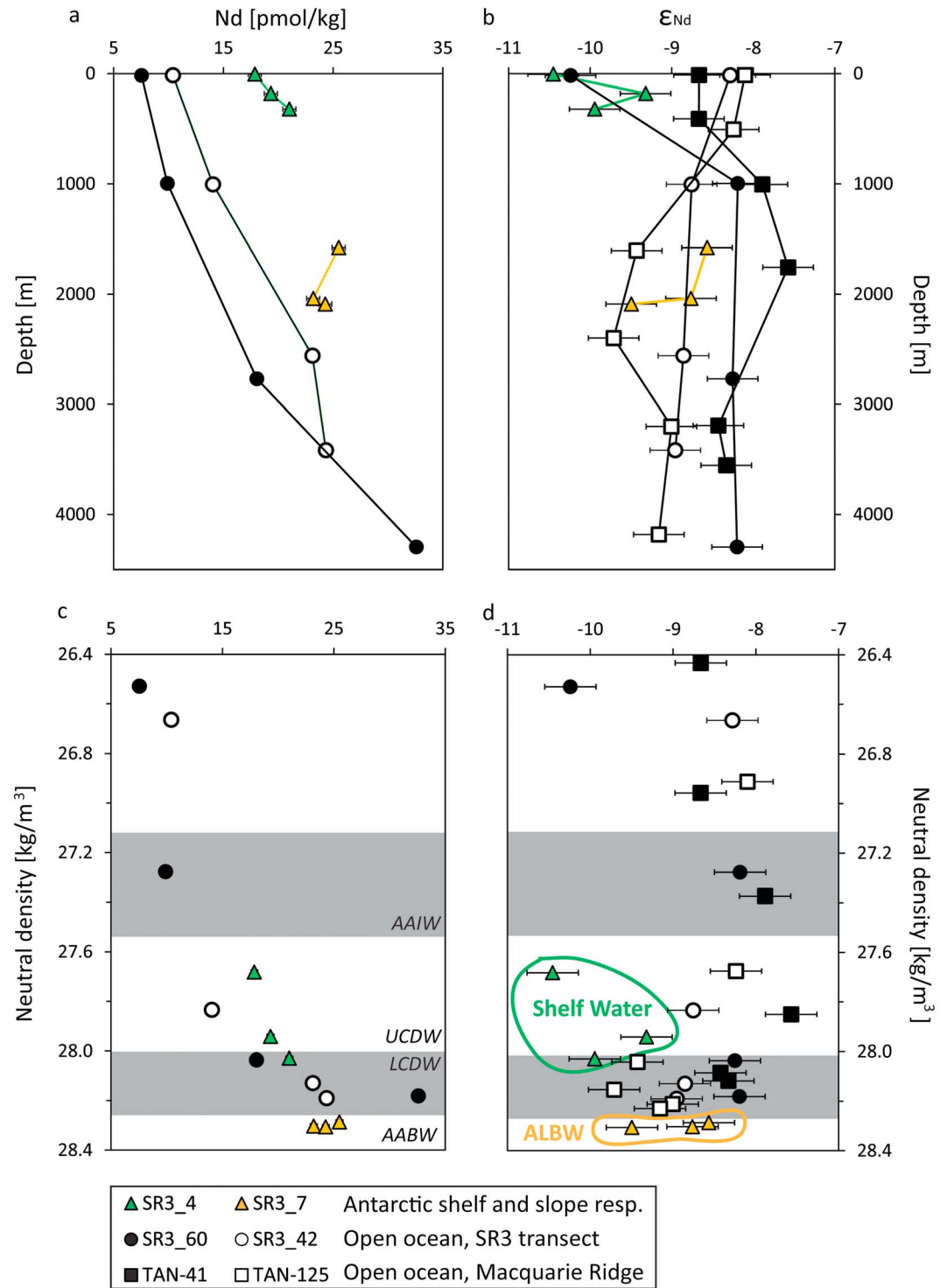


Figure 2. Neodymium concentration (a, c) and Nd isotopic composition (b, d) versus depth (a, b) and neutral density (c, d). Gray shading in panels (c) and (d) delimits the water mass boundaries. Symbol coding (representing the different areas of the present study) and water mass abbreviations as in Figure 1. Error bars represent the external 2 sigma uncertainty for repeat measurement of an in-house seawater sample ($[Nd] = \pm 0.6$ pmol/kg and $\epsilon_{Nd} = \pm 0.3$, $n = 5$).

4. Discussion

4.1. Circumpolar Water Mass Signatures in the Australian Sector of the Southern Ocean

Away from the Antarctic margin, dissolved Nd concentrations are low at the surface and overall increase with depth (Figure 2a), in agreement with previous studies from the Southern Ocean (Figure S2b; Basak et al., 2015; Carter et al., 2012; Garcia-Solsona et al., 2014; Molina-Kescher et al., 2014; Rickli et al., 2014; Stichel, Frank, Rickli, Hathorne, et al., 2012). Surface concentrations (10.4 and 7.5 pmol/kg at SR3-42 and SR3-60, respectively, Table S1 and Figures 2a and S2b) are in the range of previously observed values for Subantarctic Surface Water (north of the PF; [Nd] = 5.1 to 11.8 pmol/kg). Low Nd concentrations in open Southern Ocean surface waters can be explained by the absence of significant terrigenous input and the efficiency of Nd scavenging by biogenic particles in high productivity areas north of the SAF, as suggested by Stichel, Frank, Rickli, and Haley (2012). Increasing Nd concentrations with depth and neutral density (Figures 2a and 2c) are consistent with the idea that Nd is released upon opal dissolution with depth (Rickli et al., 2014; Stichel, Frank, Rickli, Hathorne, et al., 2012). However, similar profiles are also observed in other parts of the global ocean, where lateral processes dominate (e.g., van de Flierdt et al., 2016), and no firm conclusions can be drawn from our new low-resolution profiles regarding the control of vertical versus lateral processes in the supply of Nd to the region.

Deep and bottom water samples north of the PF were collected in the density range of UCDW and LCDW (Figure 2 and Table S1). When comparing the dissolved Nd isotopic compositions for the Australian sector of the Southern Ocean with those of the Atlantic (Jeandel, 1993; Stichel, Frank, Rickli, & Haley, 2012; Stichel, Frank, Rickli, Hathorne, et al., 2012; Garcia-Solsona et al., 2014) and Pacific (Basak et al., 2015; Carter et al., 2012; Molina-Kescher et al., 2014; Rickli et al., 2014) sectors, some conclusions can be derived (Figure S1 and Table S2).

First, our data reveal a homogenous Nd isotopic composition of UCDW ($\epsilon_{\text{Nd}} = -8.2 \pm 1.2$, $n = 3$) and LCDW ($\epsilon_{\text{Nd}} = -8.8 \pm 1.0$, $n = 10$, Figure 3a and Table S2) in the Australian sector of the Southern Ocean, supporting a uniform signature throughout the Southern Ocean (UCDW: $\epsilon_{\text{Nd}} = -8.2 \pm 0.9$, 2sd, $n = 41$; LCDW: $\epsilon_{\text{Nd}} = -8.4 \pm 1.6$, 2sd, $n = 117$; Figure 3a and Table S2). This observation has been previously made for the Atlantic and Pacific sectors (Basak et al., 2015; Garcia-Solsona et al., 2014; Stichel, Frank, Rickli, & Haley, 2012) and is confirmed by an unpaired t test revealing no significant difference in the average Nd isotopic composition of UCDW and LCDW at the 95% confidence level. The fact that Nd concentrations of LCDW are higher than those of UCDW is consistent with increasing Nd concentration with depth (Figure 2c and Table S1).

Second, even if the LCDW Nd isotope signature in the Australian sector cannot be statistically distinguished from other basins, it is notable that our LCDW data show a significant range of ~ 1.5 epsilon units, mainly due to unradiogenic values observed at 1,606- and 2,400-m water depths at station TAN-125 ($\epsilon_{\text{Nd}} = -9.4 \pm 0.3$ and $\epsilon_{\text{Nd}} = -9.7 \pm 0.3$, respectively; Figure 2b and Table S1). This station sits in close proximity to the Macquarie Ridge (Figure 1a), a relict volcanic mid-ocean ridge spreading center (Conway et al., 2012), characterized by basalts and peridotites featuring a highly radiogenic Nd isotope signature (ϵ_{Nd} from +7 to +11; Dijkstra et al., 2009; Kamenetsky et al., 2000). Thus, it is unsuitable as a potential source for the unradiogenic signal (i.e., low ϵ_{Nd}). Similarly, negative values at LCDW depths in other Southern Ocean locations have been interpreted to reflect the presence of remnants of NADW (Basak et al., 2015; Garcia-Solsona et al., 2014; Molina-Kescher et al., 2014). Sarmiento et al. (2007) showed that the NADW signature curls southward from the Atlantic sector to the Australian/Pacific sectors, so that NADW may not be seen south of the SAF in the Atlantic sector, but appears again south of Australia (see Figure 3 in Sarmiento et al., 2007 and supporting information Text S2). In the absence of any significant continental inputs to the remote location of the PF south of New Zealand, we can only speculate that the location of TAN-125 may be more susceptible to monitoring a remnant NADW signal (i.e., faster transport along the PF and hence less dilution). Higher-resolution seawater profiles are needed to unravel the origin of the unradiogenic Nd isotope fingerprint in LCDW.

4.2. The Nd Isotopic Composition of ALBW and Its Precursor Waters

Neodymium concentrations for samples close to the Antarctic shelf are generally higher than the concentrations measured at open ocean stations (Figures 2a and S2b, Table S1). This is consistent with studies in the Atlantic and Pacific sectors of the Southern Ocean and corroborates that the Antarctic shelf can act as a

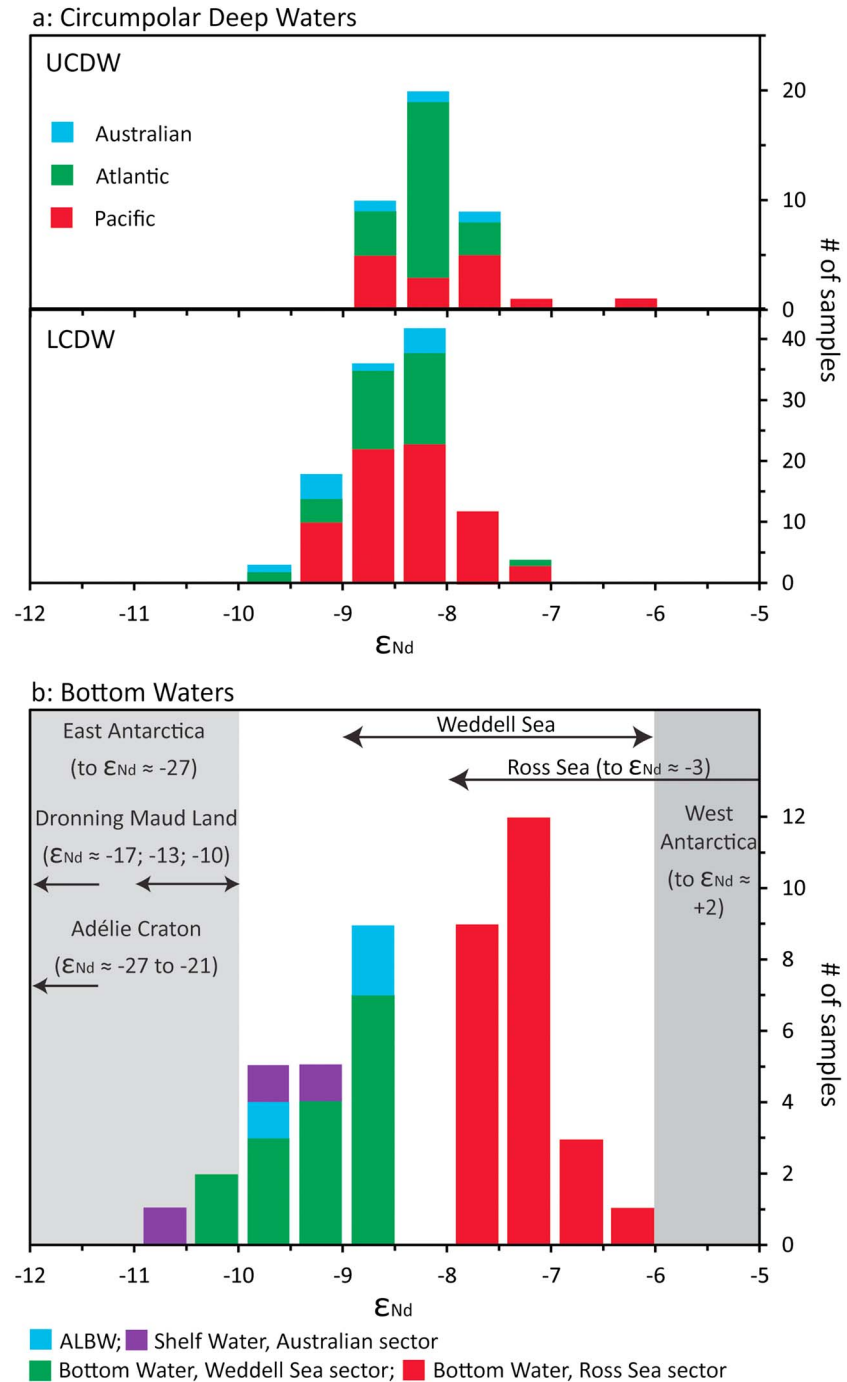


Figure 3. (a) Stacked histogram representing UCDW (upper panel) and LCDW (lower panel) ϵ_{Nd} values divided in groups of 0.5 ϵ_{Nd} units for the whole Southern Ocean. Two data points for LCDW from the Pacific sector were omitted ($\epsilon_{Nd} = -4.9$ and -3.4). Blue = Australian; green = Atlantic; red = Pacific sector. (b) Stacked histogram representing ϵ_{Nd} (divided in groups of 0.5 ϵ_{Nd} units) for bottom waters in the different sectors of the Southern Ocean south of the PF. Blue = ALBW; green = Bottom Water, Weddell Sea sector; red = Bottom Water, Ross Sea sector; purple = shelf waters, Australian sector. Arrows at the top and gray shadings: ϵ_{Nd} for detrital marine core top sediments around East Antarctica (left) and West Antarctica (right). Note the change of scale in the y axis between panels (a) and (b). Data sources: Australian sector and ALBW = this study; Atlantic and Weddell Sea sectors = Stichel, Frank, Rickli, and Haley (2012) and Garcia-Solsona et al. (2014); Pacific and Ross Sea sectors = Carter et al. (2012), Molina-Kescher et al. (2014), Rickli et al. (2014), and Basak et al. (2015); and marine sediments = van de Flierdt et al. (2006) and Roy et al. (2007). UCDW = Upper Circumpolar Deep Water; LCDW = Lower Circumpolar Deep Water; ALBW = Adélie Land Bottom Water.

source of Nd (Carter et al., 2012; Rickli et al., 2014; Stichel, Frank, Rickli, Hathorne, et al., 2012). Surface seawater at station SR3-4 is the least radiogenic measured so far in the Southern Ocean south of the PF ($\epsilon_{\text{Nd}} = -10.5 \pm 0.3$, Figure S2a and Table S1). Samples from 180- and 321-m depth at this station feature values lower than those typically observed for circumpolar waters ($\epsilon_{\text{Nd}} = -9.3 \pm 0.3$ and -9.9 ± 0.3 , Figure 3b and Table S1). Surface sediments collected on the Adélie Land Shelf feature unradiogenic detrital Nd isotope values (Figure 3b; Roy et al., 2007; van de Flierdt et al., 2007), with the nearest sediment sample showing $\epsilon_{\text{Nd}} \approx -20$ (65.55°S, 141.10°E, van de Flierdt et al., 2007). This suggests that the unradiogenic continental signature typical for the Adélie Land coast influences the Nd characteristics measured in seawater samples in the area. As all results reported here are obtained on samples collected during austral summer, they are too fresh to be classified as bottom waters. These shelf waters are, nonetheless, the precursor waters for ALBW as they get denser through brine rejection during sea ice formation in winter and form ALBW (Rintoul, 1998).

The only samples collected in the density range of bottom waters ($\gamma_n > 28.28 \text{ kg/m}^3$) were found at station SR3-7 on the Antarctic slope (Table S1 and Figures 1, 2c, 2d, 3b, S2c, and S2d), a location where the bottom water encountered is predominantly ALBW (Rintoul, 1998). The Nd isotope signature of the bottom waters is more radiogenic than the shelf waters ($\epsilon_{\text{Nd}} = -8.9 \pm 1.0$, 2sd, $n = 3$ and $\epsilon_{\text{Nd}} = -9.9 \pm 1.1$, 2sd, $n = 3$, respectively; Tables S1 and S2 and Figure 3b), but within the range of values reported for authigenic ferromanganese nodules from below 4,000 m in the Indian sector of the Southern Ocean (van de Flierdt et al., 2006).

The CFC data reveal that ALBW is composed of 25% shelf water and 75% mCDW. Using the known shelf water and ALBW Nd characteristics, the calculated Nd isotopic composition of mCDW in the area is -8.2 to -8.4 (supporting information Text S3; Mariotti et al., 1988). As these values are within error the same as LCDW (Table S2), we infer that mCDW and LCDW are similar from an isotopic point of view in the Australian sector of the Southern Ocean, even if they have different hydrographic properties. Hence, we can exclude boundary exchange as a significant process influencing these mid-depth samples in the studied area.

Our average value for ALBW ($\epsilon_{\text{Nd}} = -8.9 \pm 1.0$; $n = 3$) is similar to that of Weddell Sea Bottom Water, and both water masses are significantly less radiogenic than RSBW ($\epsilon_{\text{Nd}} \approx -7.4$; Table S2 and Figure 3b). Previous studies have shown that the Nd isotopic composition of RSBW is influenced by the radiogenic fingerprint of West Antarctic lithologies ($\epsilon_{\text{Nd}} = -6$ to $+2$, Figure 3b; Basak et al., 2015; Carter et al., 2012; Rickli et al., 2014; Roy et al., 2007; van de Flierdt et al., 2006). Similarly, newly formed Weddell Sea Bottom Water in the eastern Atlantic sector of the Southern Ocean has been shown to be influenced by inputs of unradiogenic (low ϵ_{Nd}) material from Dronning Maud Land (Garcia-Solsona et al., 2014), comprising areas of very old continental crust, similar to the Adélie Land craton (Figures 3b and S2c; Pierce et al., 2014).

We would like to note, however, that the present data set is limited ($n = 3$) and represents summer bottom water only. We hypothesize that two factors contribute to the unradiogenic signature of ALBW: the input of unradiogenic shelf waters and exchange with unradiogenic sediments as dense waters descend the continental slope, as observed in other areas around the world (Lacan & Jeandel, 2005b). Support for this hypothesis comes from considering the evolution of dissolved Nd isotope data with depth at station SR3-7, where there is a shift from $\epsilon_{\text{Nd}} = -8.8$ at 2,040 m to $\epsilon_{\text{Nd}} = -9.5$ near the seafloor at 2,090-m depth (Figure 2b and Table S1). This shift is not observed in Nd concentrations (Nd = 23.2 and 24.3 pmol/kg, respectively, Figure 2a), even though the deepest sample is located just 1 m above the seafloor. A shift of ALBW values from -8.8 to -9.5 would require a local sediment Nd isotopic composition of $\epsilon_{\text{Nd}} \approx -25$ (supporting information Text S4), which is within the range of sediments from the Adélie Craton (Pierce et al., 2014). We therefore suggest that the densest waters formed in wintertime may become even less radiogenic while cascading down the Antarctica slope margin, providing a characteristic Nd isotope fingerprint to ALBW. Sampling during wintertime, when active bottom water formation happens, would be needed to confirm this hypothesis.

5. Conclusions

Dissolved Nd isotopes and concentrations were measured at six stations in the Australian sector of the Southern Ocean. Based on its CFC content, summertime ALBW along the continental slope is composed of a mixture of shelf water (25%) and mCDW (75%). Its Nd isotopic composition of $\epsilon_{\text{Nd}} = -8.9 \pm 1.0$ (2sd,

$n = 3$) is lower than that of RSBW and similar to Weddell Sea Bottom Water. The shelf waters that contribute to ALBW are distinctly unradiogenic ($\epsilon_{\text{Nd}} = -9.9 \pm 1.1$, 2sd, $n = 3$), supporting the hypothesis that the isotopic signature of bottom waters reflects the characteristics of the local geology in the source region. In contrast, the composition of CDW is rather uniform throughout the Southern Ocean (UCDW: $\epsilon_{\text{Nd}} = -8.2 \pm 0.9$, 2sd, $n = 41$; LCDW: $\epsilon_{\text{Nd}} = -8.4 \pm 1.6$, 2sd, $n = 117$). Wintertime data capturing active formation and export of ALBW (and other varieties of AABW), as well as higher-resolution sampling along Southern Ocean transects for trace metals and isotopes, should be the target of future efforts to fingerprint bottom waters and thereby elucidate their role in the overturning circulation, now and in the past.

Acknowledgments

All data can be found in supporting information Tables S1 and S2. The scientific party and crew of the RSV *Aurora Australis* and RV *Tangaroa* during the IPY CASO-GEOTRACES SR3 and the MacRidge 2, TAN 0803 voyages are thanked, along with all members of the MAGIC group, especially Katharina Kreissig and Barry Coles, for their support in the lab. Hydrographic data from the SR3 cruise can be found in the GEOTRACES Intermediate Data Product 2014 (Mawji et al., 2015) and Nd isotopic and concentration data from the SR3 cruise in the IDP2017 (Schlitzer et al., 2018). We would like to thank two anonymous reviewers and Editor T. Ilyina for their constructive comments. The authors acknowledge funding from the NERC grant NE/J021636/1 to M. L. and T. v. d. F., the Australian Government's Cooperative Research Centre (CRC) Program through the Antarctic Climate and Ecosystems to A. B., T. R., E. B., and S. R., the National Environmental Science Program Earth System and Climate Change Hub to S. R., and the European Research Council to L. F. R.. There are no competing financial interests.

References

- Aoki, S., Rintoul, S. R., Ushio, S., Watanabe, S., & Bindoff, N. L. (2005). Freshening of the Adélie Land Bottom Water near 140°E. *Geophysical Research Letters*, 32, C12022. <https://doi.org/10.1029/2005GL024246>
- Auro, M. E., Robinson, L. F., Burke, A., Bradtmiller, L. I., Fleisher, M. Q., & Anderson, R. F. (2012). Improvements to 232-thorium, 230-thorium, and 231-protactinium analysis in seawater arising from GEOTRACES intercalibration. *Limnology and Oceanography: Methods*, 10(7), 464–474. <https://doi.org/10.4319/lom.2012.10.464>
- Basak, C., Pahnke, K., Frank, M., Lamy, F., & Gersonde, R. (2015). Neodymium isotopic characterization of Ross Sea Bottom Water and its advection through the southern South Pacific. *Earth and Planetary Science Letters*, 419, 211–221. <https://doi.org/10.1016/j.epsl.2015.03.011>
- Carter, P., Vance, D., Hillenbrand, C. D., Smith, J. A., & Shoosmith, D. R. (2012). The neodymium isotopic composition of waters masses in the eastern Pacific sector of the Southern Ocean. *Geochimica et Cosmochimica Acta*, 79, 41–59. <https://doi.org/10.1016/j.gca.2011.11.034>
- Chiswell, S. M., Bostock, H. C., Sutton, P. J. H., & Williams, M. J. M. (2015). Physical oceanography of the deep seas around New Zealand: A review, New Zeal. *Journal of Marine and Freshwater Research*, 49(2), 286–317. <https://doi.org/10.1080/00288330.2014.992918>
- Conway, C. E., Bostock, H. C., Baker, J. A., Wysoczanski, R. J., & Verdier, A. (2012). Evolution of Macquarie Ridge Complex seamounts: Implications for volcanic and tectonic processes at the Australia-Pacific plate boundary south of New Zealand. *Marine Geology*, 295–298, 34–50. <https://doi.org/10.1016/j.margeo.2011.11.009>
- Crocket, K. C., Lambelet, M., van de Fliedert, T., Rehkämper, M., & Robinson, L. F. (2014). Measurement of fossil deep-sea coral Nd isotopic compositions and concentrations by TIMS as NdO^+ , with evaluation of cleaning protocols. *Chemical Geology*, 374–375, 128–140.
- Dijkstra, A. H., Sergeev, D. S., Spandler, C. A., Pettke, T., Meisel, T., & Cawood, P. A. (2009). Highly refractory peridotites on Macquarie Island and the case for anciently depleted domains in the Earth's mantle. *Journal of Petrology*, 51(1–2), 469–493. <https://doi.org/10.1093/ptrology/egp084>
- Fukamachi, Y., Rintoul, S. R., Church, J. A., Aoki, S., Sokolov, S., Rosenberg, M. A., & Wakatsuchi, M. (2010). Strong export of Antarctic Bottom Water east of the Kerguelen plateau. *Nature Geoscience*, 3(5), 327–331. <https://doi.org/10.1038/ngeo842>
- Garcia-Solsona, E., Jeandel, C., Labatut, M., Lacan, F., Vance, D., Chavagnac, V., & Pradoux, C. (2014). Rare earth elements and Nd isotopes tracing water mass mixing and particle-seawater interactions in the SE Atlantic. *Geochimica et Cosmochimica Acta*, 125, 351–372. <https://doi.org/10.1016/j.gca.2013.10.009>
- Gordon, A. L., & Tchernia, P. L. (1978). Waters of the continental margin off Adélie Coast, Antarctica. In D. E. Hayes (Ed.), *Antarctica oceanology II: The Australian–New Zealand sector* (Vol. 19, pp. 59–69). Washington, DC: American Geophysical Union.
- Hartin, C. A., Fine, R. A., Sloyan, B. M., Talley, L. D., Chereskin, T. K., & Happell, J. (2011). Formation rates of Subantarctic mode water and Antarctic intermediate water within the South Pacific. *Deep Sea Research Part I*, 58(5), 524–534. <https://doi.org/10.1016/j.dsr.2011.02.010>
- Jacobsen, S. B., & Wasserburg, G. J. (1980). Sm–Nd evolution of chondrites. *Earth and Planetary Science Letters*, 50, 139–155. [https://doi.org/10.1016/0012-821X\(80\)90125-9](https://doi.org/10.1016/0012-821X(80)90125-9)
- Jeandel, C. (1993). Concentration and isotopic composition of Nd in the South Atlantic Ocean. *Earth and Planetary Science Letters*, 117(3–4), 581–591. [https://doi.org/10.1016/0012-821X\(93\)90104-H](https://doi.org/10.1016/0012-821X(93)90104-H)
- Kamenetsky, V. S., Everard, J. L., Crawford, A. J., Varne, R., Eggins, S. M., & Lanyon, R. (2000). Enriched end-member of primitive MORB melts: Petrology and geochemistry of glasses from Macquarie Island (SW Pacific). *Journal of Petrology*, 41(3), 411–430. <https://doi.org/10.1093/ptrology/41.3.411>
- Lacan, F., & Jeandel, C. (2005a). Acquisition of the neodymium isotopic composition of the North Atlantic Deep Water. *Geochemistry, Geophysics, Geosystems*, 6, Q12008. <https://doi.org/10.1029/2005GC000956>
- Lacan, F., & Jeandel, C. (2005b). Neodymium isotopes as a new tool for quantifying exchange fluxes at the continent–ocean interface. *Earth and Planetary Science Letters*, 232(3–4), 245–257. <https://doi.org/10.1016/j.epsl.2005.01.004>
- Lambelet, M., van de Fliedert, T., Crocket, K., Rehkämper, M., Kreissig, K., Coles, B., et al. (2016). Neodymium isotopic composition and concentration in the western North Atlantic Ocean: Results from the GEOTRACES GA02 section. *Geochimica et Cosmochimica Acta*, 177, 1–29. <https://doi.org/10.1016/j.gca.2015.12.019>
- Mantyla, A. W., & Reid, J. L. (1995). On the origins of deep and bottom waters of the Indian Ocean. *Journal of Geophysical Research*, 100(C2), 2417–2439. <https://doi.org/10.1029/94JC02564>
- Marinov, I., Gnanadesikan, A., Toggweiler, J. R., & Sarmiento, J. L. (2006). The Southern Ocean biogeochemical divide. *Nature*, 441(7096), 964–967. <https://doi.org/10.1038/nature04883>
- Mariotti, A., Landreau, A., & Simon, B. (1988). ^{15}N isotope biogeochemistry and natural denitrification process in groundwater: Application to the chalk aquifer of northern France. *Geochimica et Cosmochimica Acta*, 52(7), 1869–1878. [https://doi.org/10.1016/0016-7037\(88\)90010-5](https://doi.org/10.1016/0016-7037(88)90010-5)
- Marshall, J., & Speer, K. (2012). Closure of the meridional overturning circulation through Southern Ocean upwelling. *Nature Geoscience*, 5(3), 171–180. <https://doi.org/10.1038/ngeo1391>
- Mawji, E., Schlitzer, R., Dodas, E. M., Abadie, C., Abouchami, W., Anderson, R. F., et al. (2015). The GEOTRACES intermediate data product 2014 The GEOTRACES Group. *Marine Chemistry*, 177, 1–8. <https://doi.org/10.1016/j.marchem.2015.04.005>
- Molina-Kescher, M., Frank, M., & Hathorne, E. (2014). South Pacific dissolved Nd isotope compositions and rare earth element distributions: Water mass mixing versus biogeochemical cycling. *Geochimica et Cosmochimica Acta*, 127, 171–189. <https://doi.org/10.1016/j.gca.2013.11.038>
- Nakano, H., & Sugimotohara, N. (2002). Importance of the eastern Indian Ocean for the abyssal Pacific. *Journal of Geophysical Research*, 107(C12), 3219. <https://doi.org/10.1029/2001JC001065>

- Ohshima, K. I., Fukamachi, Y., Williams, G. D., Nihashi, S., Roquet, F., Kitade, Y., et al. (2013). Antarctic Bottom Water production by intense sea-ice formation in the Cape Darnley polynya. *Nature Geoscience*, 6(3), 235–240. <https://doi.org/10.1038/ngeo1738>
- Orsi, A. H., Johnson, G. C., & Bullister, J. L. (1999). Circulation, mixing, and production of Antarctic Bottom Water. *Progress in Oceanography*, 43(1), 55–109. [https://doi.org/10.1016/S0079-6611\(99\)00004-X](https://doi.org/10.1016/S0079-6611(99)00004-X)
- Orsi, A. H., Whitworth, T. I., & Worth, N. D. J. (1995). On the meridional extent and fronts of the Antarctic Circumpolar Current. *Deep-Sea Research Part I*, 42(5), 641–673. [https://doi.org/10.1016/0967-0637\(95\)00021-W](https://doi.org/10.1016/0967-0637(95)00021-W)
- Piepgas, D. J., & Wasserburg, G. J. (1982). Isotopic composition of neodymium in waters from the Drake Passage. *Science*, 217(4556), 207–214. <https://doi.org/10.1126/science.217.4556.207>
- Pierce, E. L., Hemming, S. R., Williams, T., van de Flierdt, T., Thomson, S. N., Reiners, P. W., et al. (2014). A comparison of detrital U-Pb zircon, $^{40}\text{Ar}/^{39}\text{Ar}$ hornblende, $^{40}\text{Ar}/^{39}\text{Ar}$ biotite ages in marine sediments off East Antarctica: Implications for the geology of subglacial terrains and provenance studies. *Earth-Science Reviews*, 138, 156–178. <https://doi.org/10.1016/j.earscirev.2014.08.010>
- Rickli, J., Gutjahr, M., Vance, D., Fischer-Gödde, M., Hillenbrand, C.-D., & Kuhn, G. (2014). Neodymium and hafnium boundary contributions to seawater along the West Antarctic continental margin. *Earth and Planetary Science Letters*, 394, 99–110. <https://doi.org/10.1016/j.epsl.2014.03.008>
- Rintoul, S. R. (1998). On the origin and influence of Adélie Land Bottom Water. In *Ocean, ice, and atmosphere: Interactions at the Antarctic continental margin* (Vol. 75, pp. 151–171). Washington, DC: American Geophysical Union.
- Rintoul, S. R. (2018). The global influence of localized dynamics in the Southern Ocean. *Nature*, 558(7709), 209–218. <https://doi.org/10.1038/s41586-018-0182-3>
- Rintoul, S. R., & Bullister, J. L. (1999). A late winter hydrographic section from Tasmania to Antarctica. *Deep Sea Research Part I: Oceanographic Research Papers*, 46(8), 1417–1454. [https://doi.org/10.1016/S0967-0637\(99\)00013-8](https://doi.org/10.1016/S0967-0637(99)00013-8)
- Rintoul, S. R., Hughes, C., & Olbers, D. (2001). The Antarctic circumpolar current system. In G. Siedler, J. Church, & J. Gould (Eds.), *Ocean circulation and climate* (pp. 271–302). New York: Academic Press.
- Rintoul, S. R., Sokolov, S., Williams, M. J. M., Peña Molino, B., Rosenberg, M., & Bindoff, N. L. (2014). Antarctic Circumpolar Current transport and barotropic transition at Macquarie Ridge. *Geophysical Research Letters*, 41, 7254–7261. <https://doi.org/10.1002/2014GL061880>
- Roy, M., van de Flierdt, T., Hemming, S. R., & Goldstein, S. L. (2007). $^{40}\text{Ar}/^{39}\text{Ar}$ Ar ages of hornblende grains and bulk Sm/Nd isotopes of circum-Antarctic glacio-marine sediments: Implications for sediment provenance in the southern ocean. *Chemical Geology*, 244(3–4), 507–519. <https://doi.org/10.1016/j.chemgeo.2007.07.017>
- Sarmiento, J. L., Simeon, J., Gnanadesikan, A., Gruber, N., Key, R. M., & Schlitzer, R. (2007). Deep ocean biogeochemistry of silicic acid and nitrate. *Global Biogeochemical Cycles*, 21, GB1590. <https://doi.org/10.1029/2006GB002720>
- Schlitzer, R. (2012). Ocean data view. Retrieved from odv.awi.de. <https://doi.org/10.1182/blood-2012-03-418400>
- Schlitzer, R., Anderson, R. F., Masferrer, E., Lohan, M., Daniels, C., Dehairs, F., et al. (2018). The GEOTRACES Intermediate Data Product 2017. *Chemical Geology*, 493, 210–223. <https://doi.org/10.1016/j.chemgeo.2018.05.040>
- Sloyan, B. M., & Rintoul, S. R. (2001). Circulation, renewal, and modification of Antarctic Mode and Intermediate Water. *Journal of Physical Oceanography*, 31(4), 1005–1030. [https://doi.org/10.1175/1520-0485\(2001\)031<1005:CRAMOA>2.0.CO;2](https://doi.org/10.1175/1520-0485(2001)031<1005:CRAMOA>2.0.CO;2)
- Smith, R. O., Vennell, R., Bostock, H. C., & Williams, M. J. M. (2013). Interaction of the subtropical front with topography around southern New Zealand. *Deep Sea Research Part I*, 76, 13–26. <https://doi.org/10.1016/j.dsr.2013.02.007>
- Sokolov, S., & Rintoul, S. R. (2002). Structure of Southern Ocean fronts at 140°E. *Journal of Marine Systems*, 37(1–3), 151–184. [https://doi.org/10.1016/S0924-7963\(02\)00200-2](https://doi.org/10.1016/S0924-7963(02)00200-2)
- Sokolov, S., & Rintoul, S. R. (2007). Multiple jets of the Antarctic Circumpolar Current south of Australia. *Journal of Physical Oceanography*, 37(5), 1394–1412. <https://doi.org/10.1175/JPO3111.1>
- Sokolov, S., & Rintoul, S. R. (2009). Circumpolar structure and distribution of the Antarctic Circumpolar Current fronts: 1. Mean circumpolar paths. *Journal of Geophysical Research*, 114, C11018. <https://doi.org/10.1029/2008JC005108>
- Stichel, T., Frank, M., Rickli, J., & Haley, B. A. (2012). The hafnium and neodymium isotope composition of seawater in the Atlantic sector of the Southern Ocean. *Earth and Planetary Science Letters*, 317–318, 282–294. <https://doi.org/10.1016/j.epsl.2011.11.025>
- Stichel, T., Frank, M., Rickli, J., Hathorne, E. C., Haley, B. A., Jeandel, C., & Pradoux, C. (2012). Sources and input mechanisms of hafnium and neodymium in surface waters of the Atlantic sector of the Southern Ocean. *Geochimica et Cosmochimica Acta*, 94, 22–37. <https://doi.org/10.1016/j.gca.2012.07.005>
- Struve, T., van de Flierdt, T., Robinson, L. F., Bradtmiller, L. I., Hines, S. K., Adkins, J. F., et al. (2016). Neodymium isotope analyses after combined extraction of actinide and lanthanide elements from seawater and deep-sea coral aragonite. *Geochemistry, Geophysics, Geosystems*, 16, 2775–2795. <https://doi.org/10.1002/2015GC005918>
- Tanaka, T., Togashi, S., Kamioka, H., Amakawa, H., Kagami, H., Hamamoto, T., et al. (2000). JNdi-1: A neodymium isotopic reference in consistency with LaJolla neodymium. *Chemical Geology*, 168(3–4), 279–281. [https://doi.org/10.1016/S0009-2541\(00\)00198-4](https://doi.org/10.1016/S0009-2541(00)00198-4)
- Tomczak, M., & Godfrey, J. S. (2005). Antarctic oceanography. In *Regional oceanography: an introduction* (Vol. 1, pp. 63–82). London: Butler & Tanner Ltd.
- van de Flierdt, T., Goldstein, S. L., Hemming, S. R., Roy, M., Frank, M., & Halliday, A. N. (2007). Global neodymium–hafnium isotope systematics —Revisited. *Earth and Planetary Science Letters*, 259(3–4), 432–441. <https://doi.org/10.1016/j.epsl.2007.05.003>
- van de Flierdt, T., Griffiths, A. M., Lambelet, M., Little, S. H., Stichel, T., & Wilson, D. J. (2016). Neodymium in the oceans: A global database, a regional comparison and implications for palaeoceanographic research. *Philosophical Transactions of the Royal Society A*, 374, 1–30.
- van de Flierdt, T., Hemming, S. R., Goldstein, S. L., & Abouchami, W. (2006). Radiogenic isotope fingerprint of Wilkes Land–Adélie Coast Bottom Water in the circum-Antarctic Ocean. *Geophysical Research Letters*, 33, L12606. <https://doi.org/10.1029/2006GL026020>
- van Wijk, E. M., & Rintoul, S. R. (2014). Freshening drives contraction of Antarctic Bottom Water in the Australian Antarctic Basin. *Geophysical Research Letters*, 41, 1657–1664. <https://doi.org/10.1002/2013GL058954>
- Whitworth, T. I., Orsi, A. H., Kim, S.-J., Nowlin, W. D. J., & Locarnini, R. A. (1998). Water masses and mixing near the Antarctic slope front. In *Ocean, ice, and atmosphere: Interactions at the Antarctic continental margin* (Vol. 75, pp. 1–27). Washington, DC: American Geophysical Union.
- Williams, G. D., Aoki, S., Jacobs, S. S., Rintoul, S. R., Tamura, T., & Bindoff, N. L. (2010). Antarctic bottom water from the Adélie and George V Land Coast, East Antarctica (140–149°E). *Journal of Geophysical Research*, 115, C04027. <https://doi.org/10.1029/2009JC005812>